Available online at www.sciencedirect.com

ScienceDirect

Energy Procedia 92 (2016) 419 – 426

Energy Procedia

6th International Conference on Silicon Photovoltaics, SiliconPV 2016

Development of n-type selective emitter silicon solar cells by laser doping using boron-doped silicon paste

Yuka Tomizawa[a,*], Yoshinori Ikeda[a], Takashi Shiro[a,b]

[a]*Teijin Limited, 4-3-2, Asahigaoka, Hino, Tokyo 191-8512, Japan*
[b]*NanoGram Corporation, 165 Topaz Street, Milpitas, California 95035, USA*

Abstract

N-type solar cells are being developed as next generation photovoltaic solar cells, and have attracted a significant amount of attention. In addition, the demand for high-efficiency silicon solar cells has increased in order to reduce production costs and save space. In this study, we demonstrate boron laser doping (LD) using a boron-doped NanoGram® Si paste in n-type passivated emitter, rear totally diffused solar cells. The sheet resistance was 54 Ω/sq at the local boron emitter after boron LD. The boron diffusion depth was ~2.0 μm, and the boron surface concentration was 7×10^{19} atoms/cm^3. The n-type solar cells were fabricated using boron LD to have front side boron selective emitters. The characteristics of the newly developed solar cells improved in comparison with those of the reference cells (i.e., those without boron selective emitters), and a maximum efficiency of 19.70% was achieved. The improved efficiency was mainly due to the increase in the short circuit current density and fill factor.

Peer review by the scientific conference committee of SiliconPV 2016 under responsibility of PSE AG.

Keywords: Si nanoparticles; Solar cell; Laser doping

1. Introduction

Laser doping (LD) in solar cells is a promising technique, as it is advantageous in terms of atmospheric room-temperature processing, achieving easy control over the doping depth and concentration, and controlling the pattern of the doping area without lithography. In recent developments of solar cells, laser technology has been used for the

* Corresponding author. Tel.: +81-42-586-8594; fax: +81-42-587-5510.
E-mail address: y.tomizawa@teijin.co.jp

Peer review by the scientific conference committee of SiliconPV 2016 under responsibility of PSE AG.
doi:10.1016/j.egypro.2016.07.122

selective emitter (SE) [1, 2], passivated emitter, rear contact (PERC) [3], and passivated emitter, rear locally diffused (PERL) cells. PERL cells with over 20% efficiency that are fabricated using the LD method have been reported [4-6]. As next-generation high-efficiency solar cells, n-type solar cells are attracting an increasing amount of attention [7-9]. N-type solar cells offer advantages such as high cell efficiency and performance based on long lifetimes and low amounts of light degradation compared with p-type solar cells. Because boron exists in the p-type wafer, boron-oxygen defects are formed by light irradiation, and light degradation occurs [10].

In order to achieve high cell efficiency in n-type solar cells, it is important for n-type solar cells to have local diffusion areas similar to those of p-type solar cells. However, there are few reports on the fabrication of a local boron diffusion area for n-type solar cells using the LD method. Also, the effect of the local boron diffusion area on the performance of n-type solar cells is not clearly understood.

In this study, we fabricated n-type passivated emitter, rear totally diffused (PERT) solar cells with and without the local boron diffusion area as boron SEs by LD using boron-doped NanoGram® Si paste, and evaluated the cell characteristics.

2. Experiments

The schematic cross-sectional views of the fabricated solar cells are shown in Fig. 1. Groups A and B without boron SEs functioned as reference cells (Fig. 1(a)), whereas group C consisted of n-PERT solar cells with boron SEs fabricated by LD using boron-doped Si paste on the front side (Fig. 1(b)).

Figure 2 describes the fabrication process of the n-PERT solar cells. The 50 mm × 50 mm cells were processed on n-type Si wafers with a thickness of 200 ± 30 μm. BBr_3 diffusion was performed following an alkali texturing process. A diffusion barrier was formed on the rear side before BBr_3 diffusion to prevent the diffusion of boron to the rear side. The sheet resistance after BBr_3 diffusion was 90 ± 5 Ω/sq. The diffusion barrier was removed after BBr_3 diffusion, which was followed by the formation of a phosphorus diffusion barrier on the front side. $POCl_3$ diffusion was carried out on the rear side in order to form a back surface field. A passivation layer was deposited on the front and rear sides by plasma-enhanced chemical vapor deposition. Boron-doped Si paste (NanoGram Corp. nSol-32113) was used as a printable boron-doped material.

The LD method is schematically presented in Fig. 3. The Si paste was printed on the front side and dried at 200 °C after deposition of the passivation layer in Group C in order to form a Si paste layer with a thickness of approximately 2 μm. A 532 nm Q-switched pulsed laser was used for LD. The local boron diffusion area was obtained by irradiating the Si paste layer with the laser. The cells were contacted by screen-printing Ag paste on the rear side and Al/Ag paste on the front side. Two electrodes were printed and fired separately from each other. In Group A, the cells were co-fired after printing the electrode on the front and rear sides. In Group B, the electrode was formed by the same method that was used for Group C, which was followed by laser irradiation in order to create contact holes in the passivation layer.

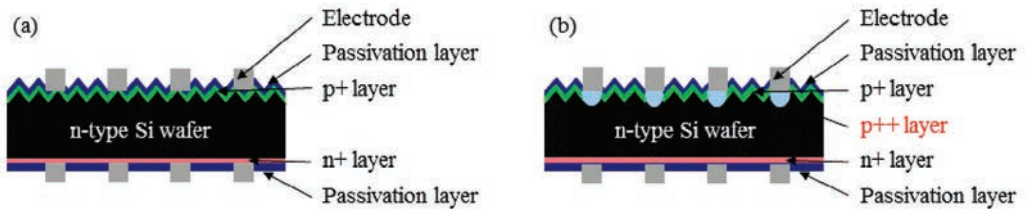

Fig. 1. Schematic cross-sectional view of n-type PERT solar cells. (a) Groups A and B without the local boron diffusion area (p++ layer), which were used as the reference. (b) Group C with a local boron diffusion area (p++ layer), which functioned as boron SEs.

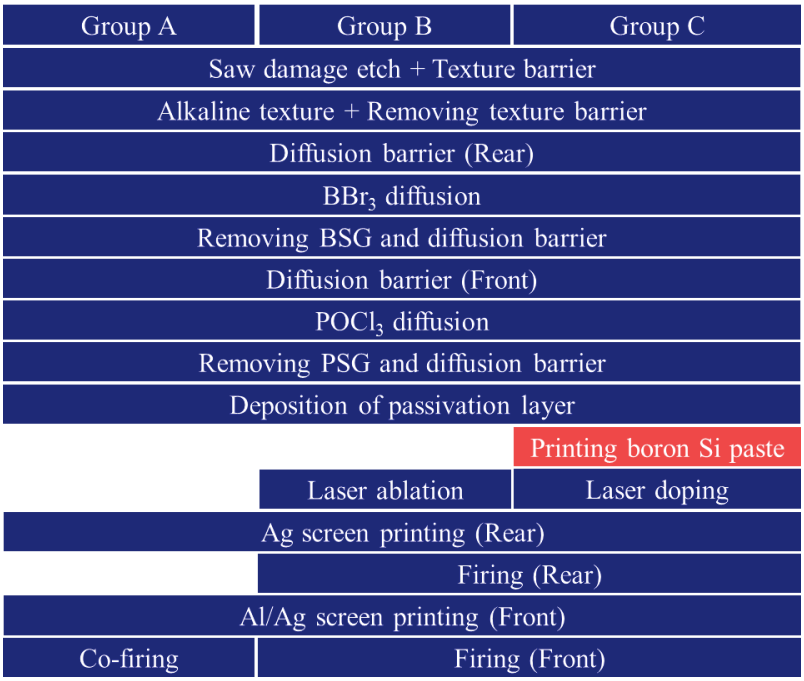

Fig. 2. Fabrication process of n-type PERT solar cells with and without boron SEs.

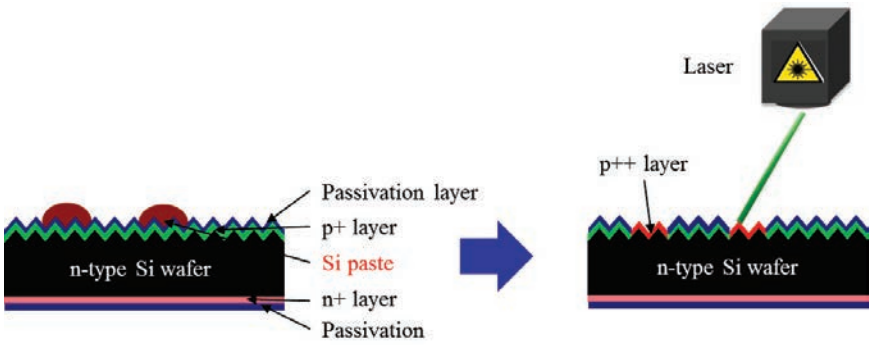

Fig. 3. Schematic diagram of the LD method using boron-doped Si paste.

3. Results and discussion

3.1. Laser doping properties

The printing state of boron-doped Si paste after screen printing was observed using a scanning electron microscope (SEM). It was observed that boron-doped Si paste fully covered the textured wafer (Fig. 4). The sheet resistance of the boron LD area was measured using the four-point probe method (Fig. 5). As the laser fluence and overlap ratio increased, the sheet resistance decreased. The sheet resistance of the front side was 54 Ω/sq at a laser fluence of 2.0 J/cm^2 and an overlap ratio of 90%. Figure 6 shows the depth profile of boron concentration obtained using secondary ion mass spectrometry (SIMS) analysis. The diffusion depth of the boron dopant can be controlled by adjusting the laser power. At a laser fluence of 2.0 J/cm^2 and an overlap ratio of 90%, the boron dopant depth was approximately 2.0 μm, and the boron surface concentration was 7×10^{19} atoms/cm^3.
The carrier distributions in n-type PERT solar cells were measured using scanning capacitance microscopy (SCM), as shown in the cross-sectional images in Fig. 7. The pn junction was observed at a depth of 1.0–1.5 μm from the surface of the textured wafer before LD. The p++ layer was formed at a depth of 2.0–2.5 μm after LD using the boron-doped NanoGram® Si paste. The SCM result corresponds to the result of boron dopant depth obtained from the SIMS analysis.

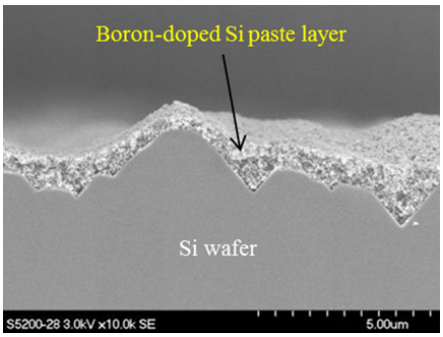

Fig. 4. SEM image of the boron-doped NanoGram® Si paste layer after screen printing.

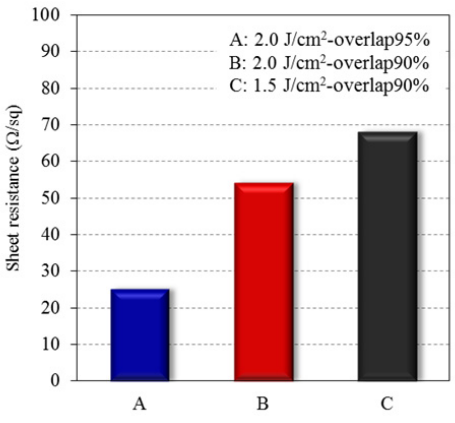

Fig. 5. Sheet resistance in the boron LD area.

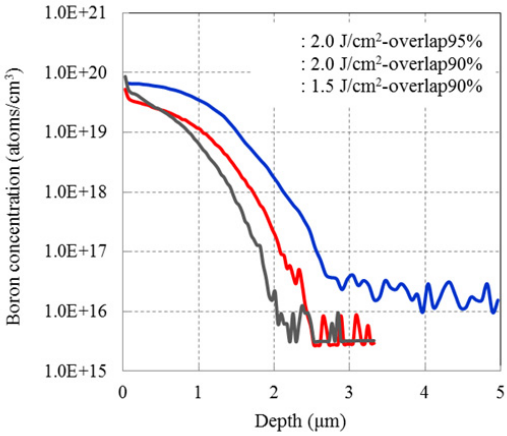

Fig. 6. Dopant depth profile of boron atoms as a function of laser irradiation conditions on the boron LD area.

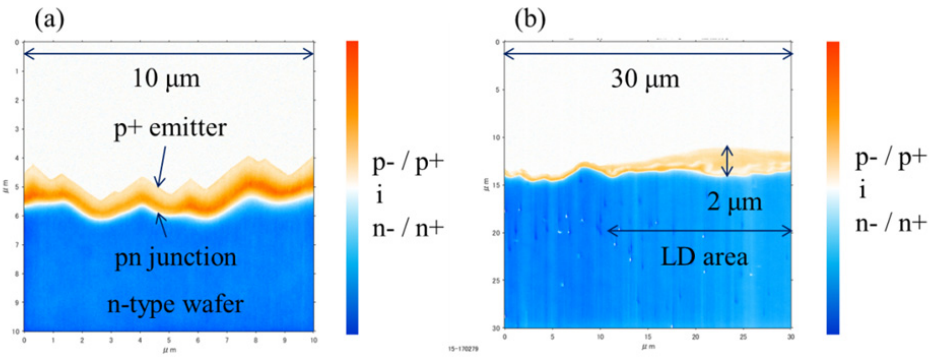

Fig. 7. Cross-sectional images of carrier distribution in n-type PERT solar cells measured using SCM. (a) p+ emitter region before LD (b) p++ emitter region after LD on the front side of the wafer.

3.2. Characteristics of the fabricated solar cells

The cell characteristics were measured using a solar simulator (Table 1). The maximum and average cell efficiencies of Group C were 19.70% and 19.55%, respectively. The efficiency of Group C with boron SEs was higher those of Groups A and B without boron SEs. The highest cell efficiency was obtained for a sheet resistance of 54 Ω/sq after LD. The primary improvements in the cell performance concerned the short circuit current density (Jsc) and fill factor (FF).

It has been reported that selective emitters benefit from less Auger recombination, less contact recombination, and lower contact resistivity [11]. When boron SEs are formed in solar cells and the doping concentration of the emitter layer is reduced, Auger recombination is diminished, and the solar cell characteristics (in particular, the open-circuit voltage (Voc)) are improved. The high-concentration dopant layer of boron SEs acts as a front surface field; Voc therefore improves because of the decrease in contact recombination. Also, the high-concentration dopant layer of boron SEs leads to high Jsc by a low contact resistivity. In this study, improvements in Jsc and FF were clearly observed; however, only a slight improvement in Voc was obtained. Because boron SEs achieved a low contact resistivity, it was thought that 7×10^{19} atoms/cm^3 was sufficient for the surface concentration of boron.

However, no significant improvement in Voc could be found because the doping concentration of the emitter layer was slightly high with a sheet resistance of 90 Ω/sq. Therefore, it is necessary to optimize the dopant concentration of the emitter and the doping profile of boron SEs in order to further improve the boron SE solar cells.
The current-voltage curve and internal quantum efficiency (IQE) of the newly developed n-PERT solar cell with boron SEs are shown in Figs. 8 and 9, respectively. The IQE exhibits an impressive response across a wide range of wavelengths. It is assumed that the blue response of IQE can be improved by optimizing the dopant concentration of the emitter and the doping profile of boron SEs.

Table 1. Solar cell characteristics of Groups A-C.

Cell type		V_{oc} (V)	J_{sc} (mA/cm^2)	*FF* (%)	η (%)
Group A	Av.	0.645	38.73	74.7	18.66
	Max	0.646	38.80	74.7	18.71
Group B	Av.	0.654	38.30	76.9	19.26
	Max	0.654	38.42	77.8	19.57
	Suns-Voc	0.647	38.30	81.0	20.08
Group C	Av.	0.656	38.46	77.5	19.55
	Max	0.655	38.59	77.9	19.70
	Suns-Voc	0650	38.46	81.4	20.35

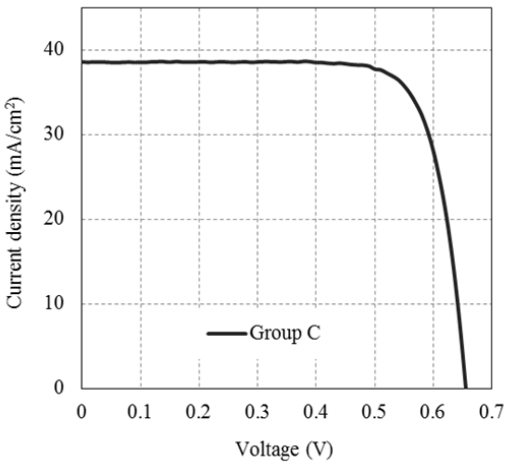

Fig. 8. Current-voltage curve of the newly developed n-PERT solar cell with boron SEs.

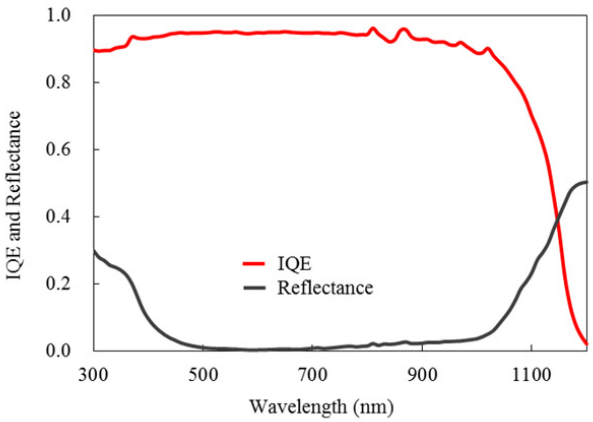

Fig. 9. IQE and reflectance curves of the newly developed n-PERT solar cell with boron SEs.

4. Conclusion

We developed an n-PERT solar cell with boron SEs using LD and boron-doped NanoGram® Si paste. The LD using a boron-doped NanoGram® Si paste facilitated the fabrication of boron SEs in a simple processing step. We were able to control the doping depth profile by varying the laser irradiation conditions. The newly developed n-PERT solar cell provides a maximum efficiency of up to 19.70%, which represents an improvement of ~0.3% in comparison with the efficiency of the reference cells. Moreover, the improvements in Jsc and FF were remarkable. The results demonstrate that 7×10^{19} atoms/cm^3 was sufficient for the surface concentration of boron, as the boron SEs reduced the contact resistivity. On the other hand, only a slight improvement in Voc was obtained. Further characteristic improvements can be expected by optimizing the dopant concentration of the emitter and the doping profile of the boron SEs.

Acknowledgements

We would like to thank ROFIN-BAASEL Japan Corporation for laser doping.

Reference

[1] Paviet-Salomon B, Gall S, Monna R, Manuel S, Slaoui A. Analysis of laser-doped phosphorus emitters. Energy Procedia 2011;8:214-9.
[2] Isenberg J, Ehling C, Esturo-Breton A, Frieß T, Geiger M, Hanke M, Keller S, Kühn T, Melnyk I, Olkowska-Oetzel J, Sterk S, Teppe A, Varner K, Winter P, Finck C, Bopp B, Hendel R, Mayerhofer R, Geiger S, Zhang W, Huang L, Fath P. Laser diffused selective emitters with efficiencies above 18.5% in industrial production. 26th European Photovoltaic Solar Energy Conference 2011;890.
[3] Hallam B, Urueñ A, Russell R, Aleman M, Abbott M, Dang C, Wenham S, Tous L, Poortmans J. Efficiency enhancement of i-PERC solar cell by implementation of a laser doped selective emitter. Sol Energ Mat Sol Cells 2015;134:89-98.
[4] Tomizawa Y, Imamura T, Soeda M, Ikeda Y, Shiro T. Laser doping of boron-doped Si paste for high efficiency silicon solar cells. Jpn J Appl Phys 2015;54:08KD06.
[5] Jäger U, Wolf A, Wufka C, Mack S, Tomizawa Y, Imamura T, Soeda M, Ikeda Y, Shiro T. Local boron doping for p-type PERL silicon solar cells fabricated by laser processing of doped silicon nanoparticle paste. 29th European Photovoltaic Solar Energy Conference 2014;1111.
[6] Gall S, Manuel S, Lerat JF. Boron laser doping through high quality Al2O3 passivation layer for localized B-BSF PERL solar cells. Energy Procedia 2013;38:270-7.
[7] Yang X, Bullock J, Bi Q, Weber K. High efficiency n-type silicon solar cells featuring passivated contact to laser doped regions. Appl Phys Lett 2015;106:113901.
[8] Chen J, Deckers J, Choulat P, Kuzma-Filipek I, Aleman M. Investigation of laser ablation on boron emitters for n-type rear-junction PERT type silicon wafer solar cells. Progr Photovolt: Res Appl 2015;23:1706-1714.

[9] Jäger U, Suwito D, Benick J, Janz S, Preu R. A laser based process for the formation of a local back surface field for n-type silicon solar cells. Thin Solid Films 2011;519:3827-3830.
[10] Schmidt J, Bothe K. Structure and transformation of the metastable boron- and oxygen-related defect center in crystalline silicon. Phys Rev B 2004;69:024107.
[11] Liu J, Janssen GJM, Koppes M, Kossen EJ, Tool K, Komatsu Y, Anker J, Gutjahr A, Vlooswijk A, Luchies JM, Siareyeva O, Granneman E, Romijn I. Selective emitter in n-type c-Si solar cells. 31st European Photovoltaic Solar Energy Conference 2015;633.